

Nuclear Spin Gyroscope Based on an Atomic Comagnetometer

T. W. Kornack, R. K. Ghosh, and M. V. Romalis

Department of Physics, Princeton University, Princeton, New Jersey 08550 USA

(Received 6 May 2005; published 29 November 2005)

We describe a nuclear spin gyroscope based on an alkali-metal–noble-gas comagnetometer. Optically pumped alkali-metal vapor is used to polarize the noble-gas atoms and detect their gyroscopic precession. Spin precession due to magnetic fields as well as their gradients and transients can be cancelled in this arrangement. The sensitivity is enhanced by using a high-density alkali-metal vapor in a spin-exchange relaxation free regime. With a K- ^3He comagnetometer we demonstrate rotation sensitivity of $5 \times 10^{-7} \text{ rad s}^{-1} \text{ Hz}^{-1/2}$, equivalent to a magnetic field sensitivity of $2.5 \text{ fT/Hz}^{1/2}$. The rotation signal can be increased by a factor of 10 using ^{21}Ne with a smaller magnetic moment. The comagnetometer is also a promising tool in searches for anomalous spin couplings beyond the standard model.

DOI: [10.1103/PhysRevLett.95.230801](https://doi.org/10.1103/PhysRevLett.95.230801)

PACS numbers: 07.07.Df, 32.80.Bx, 33.25.+k, 33.35.+r

Sensitive gyroscopes are used in many applications, from inertial navigation to studies of the Earth's rotation and tests of general relativity [1]. A variety of physical principles are utilized for rotation sensing, including mechanical sensing, the Sagnac effect for photons [1,2] and atoms [3,4], the Josephson effect in superfluid ^4He and ^3He [5], and nuclear spin precession [6]. While mechanical gyroscopes operating in a low gravity environment remain so far unchallenged [7], research continues on the development of more versatile rotation sensing techniques.

Nuclear spin gyroscopes [6] measure the shift of the NMR frequency caused by inertial rotation. At least two spin species with different gyromagnetic ratios occupying the same volume are used in a “comagnetometer” arrangement to cancel the magnetic field dependence of the NMR frequency. Spin gyroscopes have been developed using ^{129}Xe and ^{83}Kr atoms polarized by spin exchange [8] and optically pumped ^{199}Hg and ^{201}Hg isotopes [9]. More recently, similar comagnetometers have been used to search for physics beyond the standard model. For example, a ^3He - ^{129}Xe Zeeman maser pumped by spin exchange with alkali atoms has been used to search for a CP -violating electric dipole moment [10] and for a Lorentz-violating background field [11]. In both gyroscope and fundamental physics applications, the long-term stability is limited by imperfect cancellation of external magnetic fields and frequency shifts due to magnetic dipolar interactions between spins, spin-exchange collisions, and light shifts.

Here we describe a new type of alkali-metal noble-gas comagnetometer that can be used for both inertial rotation sensing and fundamental physics applications. The alkali-metal magnetometer is operated in the spin-exchange relaxation free (SERF) regime where a magnetic field sensitivity of $0.5 \text{ fT/Hz}^{1/2}$ has been demonstrated [12,13]. It would correspond to a rotation sensitivity of $1 \times 10^{-8} \text{ rad s}^{-1} \text{ Hz}^{-1/2}$ in a K- ^{21}Ne gyroscope. We show that the comagnetometer is effective in suppressing the sensitivity to magnetic fields, their gradients, and transients. Spin exchange and light shifts are also suppressed

to first order. The bandwidth and transient response of the comagnetometer are improved by dynamic damping due to coupling between noble-gas and alkali-metal spins [14]. We describe an experimental implementation of the comagnetometer using K and ^3He atoms with a short term sensitivity of $2.5 \text{ fT/Hz}^{1/2}$, approximately a factor of 100 higher than obtained in [10]. The apparatus is presently used to search for a Lorentz-violating spin coupling [15]. We also present a theoretical analysis of the comagnetometer response and derive fundamental limits for its performance.

The comagnetometer consists of a 2.5 cm diameter spherical glass cell that contains a small quantity of potassium, 7 amagat of ^3He and 20 torr of N_2 . K atoms are polarized by optical pumping and transfer the polarization to the ^3He by spin-exchange collisions. A probe laser passes through the cell perpendicular to the pump laser and measures the transverse component of the K spin polarization. The imaginary part of the K- ^3He spin-exchange cross section strongly couples the two spin ensembles. In a spherical cell this coupling can be represented by an effective magnetic field that one spin species experiences from the average magnetization of the other, $\mathbf{B} = \lambda \mathbf{M}$, where $\lambda = 8\pi\kappa_0/3$ [16] and κ_0 ranges from about 5 to 600 for different alkali-metal–noble-gas pairs [17]. The basic operation of the comagnetometer can be understood from Fig. 1. A bias magnetic field is applied parallel to the pump beam and its value is set to approximately cancel the field created by the nuclear magnetization $\lambda \mathbf{M}_n$, so the net magnetic field experienced by the K atoms is close to zero. This allows high-sensitivity SERF operation of the K magnetometer that is primarily sensitive to the B_y field. However, the nuclear magnetization adiabatically follows a slowly changing magnetic field and cancels to first order any changes in the B_y field, as shown in Fig. 1(b). Such cancellation only occurs for interactions that couple to spins in proportion to their magnetic moments, leaving the comagnetometer sensitive to inertial rotation or other anomalous spin couplings [14].

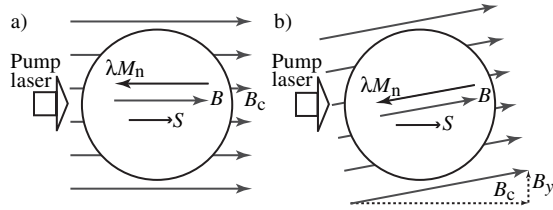


FIG. 1. Basic operation of the comagnetometer. (a) Alkali-metal and noble-gas atoms are polarized along the bias field $B_c \approx -\lambda M_n$. (b) The nuclear magnetization adiabatically follows slow changes in the external field, cancelling the effect of a small B_y field on the alkali-metal spins S .

The experimental apparatus is similar to the one used in [14]. Briefly, the comagnetometer cell is heated to 170 °C and located inside 5-layer magnetic shields. The pump laser is circularly polarized and tuned to the D1 resonance while the probe laser is linearly polarized and detuned by about 0.5 nm. The active volume defined by the intersection of the pump and probe beams is about 0.5 cm³. A Faraday modulation technique is used to measure the optical rotation of the probe beam caused by the alkali-metal atoms and a Pockels cell is used to cancel any birefringence introduced by optical elements. Feedback circuits control the wavelength and intensity of pump and probe lasers. Magnetic fields and light shifts are periodically zeroed using a modulation procedure described below. To induce rotation of the apparatus, the floating optical table is pushed with a piezo and its orientation is monitored by 6 noncontact position sensors.

As shown in [14], the comagnetometer can be described by a set of coupled Bloch equations for the electron and nuclear polarizations, \mathbf{P}^e and \mathbf{P}^n ,

$$\begin{aligned} \frac{\partial \mathbf{P}^e}{\partial t} &= \boldsymbol{\Omega} \times \mathbf{P}^e + \frac{\gamma_e}{Q(P^e)} (\mathbf{B} + \lambda M_0^n \mathbf{P}^n + \mathbf{L}) \times \mathbf{P}^e \\ &\quad + (R_p \mathbf{s}_p + R_{se}^e \mathbf{P}^n + R_m \mathbf{s}_m - R_{tot} \mathbf{P}^e) / Q(P^e), \\ \frac{\partial \mathbf{P}^n}{\partial t} &= \boldsymbol{\Omega} \times \mathbf{P}^n + \gamma_n (\mathbf{B} + \lambda M_0^e \mathbf{P}^e) \times \mathbf{P}^n \\ &\quad + R_{se}^n (\mathbf{P}^e - \mathbf{P}^n) - R_{sd}^n \mathbf{P}^n. \end{aligned} \quad (1)$$

Here $\boldsymbol{\Omega}$ is the inertial rotation rate, $\gamma_e = g_s \mu_B / \hbar$ and $\gamma_n = \mu_n / I \hbar$ are the gyromagnetic ratios of electron and nuclear spins. M_0^e and M_0^n are the magnetizations of electron and nuclear spins corresponding to full spin polarizations. \mathbf{L} is the effective magnetic field for alkali-metal spins created by the light shift from pumping and probing lasers [18]. R_p and R_m are the pumping rates of the pump and probe laser beams, while \mathbf{s}_p and \mathbf{s}_m give the directions and magnitudes of their photon spin polarizations. R_{se}^e is the alkali-metal–noble-gas spin-exchange rate for an alkali atom and R_{se}^n is the same rate for a noble-gas atom. R_{tot} is the total spin relaxation rate for alkali atoms; $R_{tot} = R_p + R_m + R_{se}^e + R_{sd}^e$, where R_{sd}^e is the electron spin destruction rate. R_{sd}^n is the nuclear spin relaxation rate. $Q(P^e)$ is the

electron slowing-down factor due to hyperfine interaction and spin-exchange collisions [13]. For alkali-metal isotopes with $I = 3/2$ in the regime of fast alkali-metal spin exchange, $Q(P^e)$ ranges from 6 for low P^e to 4 for $P^e \approx 1$.

The comagnetometer is nominally configured with the pump beam directed along the \hat{z} axis and the probe beam directed along the \hat{x} axis. The bias field is set to $\mathbf{B} = B_c \hat{z} = -(B^n + B^e) \hat{z}$. Here the effective field from nuclear magnetization $B^n = \lambda M_0^n P_z^n$ is typically on the order of a few mG and the effective field from the electron magnetization $B^e = \lambda M_0^e P_z^e$ is on the order of a few μ G. The light shifts can be set to zero, $\mathbf{L} = 0$, because the pump beam is tuned to the center of the optical resonance and the probe beam is linearly polarized. Under these conditions the gyroscope signal, proportional to the optical rotation of the probe beam due to P_x^e , is accurately given by

$$S = P_x^e = \frac{\gamma_e \Omega_y P_z^e}{\gamma_n R_{tot}} \left(1 - \frac{\gamma_n}{\gamma_e} Q(P^e) - C_{se}^n \right). \quad (2)$$

Thus, the signal is proportional to the rotation about the \hat{y} axis and is enhanced by the ratio $\gamma_e / \gamma_n \gg 1$. The nuclear spin-exchange correction factor $C_{se}^n = (\gamma_e P_z^e R_{se}^n) / (\gamma_n P_z^n R_{tot})$ is typically on the order of 10^{-3} .

Figure 2 shows the angular velocity measured by the spin gyroscope compared with the angular velocity Ω_y obtained from the position sensors. The gyroscope sensitivity is calibrated as described below and agrees with position measurements within the calibration accuracy of 3%. We also checked that the gyroscope is insensitive to the other two components of the angular velocity.

The sensitivity of the gyroscope is shown in Fig. 3. The angle random walk (ARW) is 0.002 deg/h^{1/2} or 5×10^{-7} rad s⁻¹ Hz^{-1/2} in the white noise region and corresponds to a magnetic field sensitivity of 2.5 fT/Hz^{1/2}. The low frequency angle drift of the gyroscope in the present implementation is about 0.04 deg/h.

Next we consider the effects of experimental imperfections. The only first-order dependence on the magnetic fields or light-shift fields comes from the B_x field:

$$S(B_x) = B_x P_z^e (C_{se}^e + C_{se}^n) / B^n, \quad (3)$$

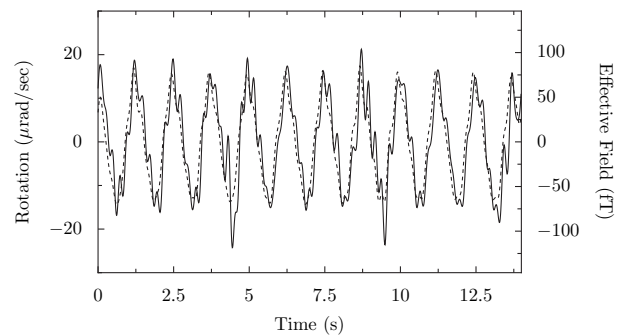


FIG. 2. Angular velocity of the optical table measured with the comagnetometer (solid line) and position sensors (dashed line), plotted with no free parameters.

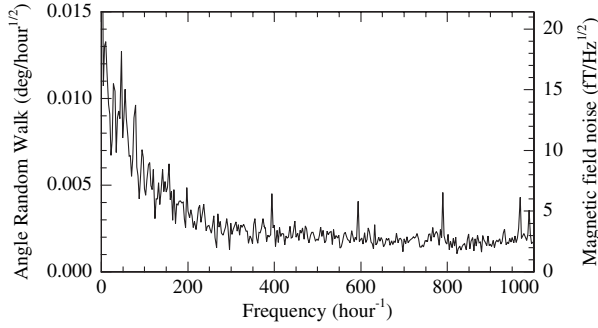


FIG. 3. Fourier spectrum of the gyroscope rotation noise. Discrete peaks are an artifact of periodic background measurements. The $1/f$ noise knee is at about 0.05 Hz.

where the electron spin-exchange correction $C_{se}^e = (R_{se}^e P_z^n)/(R_{tot} P_z^e)$ is on the order of 10^{-2} . Because electron and nuclear spin-exchange corrections are small and $R_{tot} \ll \gamma_e B^n$, this field sensitivity is suppressed by a factor of about 10^5 . Misalignment of the pump and probe beams by an angle α away from 90° gives a signal $S = \alpha R_p/R_{tot}$. For typical conditions, $1 \mu\text{rad}$ of misalignment gives a false rotation of 10^{-8} rad/s. Misalignment can be distinguished from a true rotation signal by its dependence on the pumping rate R_p . Small circular polarization of the probe laser s_m gives a first-order signal $S = s_m R_m/R_{tot}$, which can be set to zero by minimizing the probe light shift as described below.

Other imperfections only affect the signal to second order in small quantities. For example, the signal due to the B_y field is given by

$$S(B_y) = \frac{\gamma_e B_y P_z^e}{B^n R_{tot}} (B_z - (B_z + L_z) C_{se}^e - (2B_z + L_z) C_{se}^n) \quad (4)$$

where B_z is a small detuning away from the compensation field B_c . In addition to suppressing imperfections by two small factors, such second order dependence allows us to calibrate the comagnetometer and provides a mechanism for zeroing many offsets. For example, to set B_z to zero we apply a modulation to the B_y field, measure the response as a function of B_z and find the point where it vanishes. The slope of the response is given by

$$\frac{\partial^2 S}{\partial B_y \partial B_z} = \frac{\gamma_e P_z^e}{B^n R_{tot}} (1 - C_{se}^e - 2C_{se}^n) \approx \frac{\gamma_e P_z^e}{|B_c| R_{tot}}. \quad (5)$$

The approximations in the last step are accurate to better than 1% because under typical conditions $B^e \ll B^n$ and $C_{se}^e, C_{se}^n \ll 1$. The measurement of the slope gives a calibration of the gyroscope signal (2) in terms of the known applied magnetic fields B_y , B_z , and B_c . Most other field, light shift, and alignment imperfections can be minimized in a similar way with an appropriate choice of modulation. For example, a term in the signal proportional to $L_x L_z$ allows us to minimize the light shifts of the pump and

probe beams by modulating one of them and adjusting the other to get zero response. Since $L_x \propto s_m$, this also minimizes the probe circular polarization.

The transient response of the gyroscope is also improved in the comagnetometer configuration. In navigation applications, the rotation frequency is integrated over time to obtain the rotation angle. Using the Green's function for linearized Bloch equations [14], it can be shown that the integral of the signal is proportional to the total angle of inertial rotation about the \hat{y} axis independent of the time dependence of Ω_y . Furthermore, the net rotation angle generated by an arbitrary magnetic field transient is equal to zero as long as spin polarizations are rotated by a small angle during the transient. Figure 4 shows the experimental response of the gyroscope to a transient magnetic field spike, demonstrating reduction of the spin rotation angle by a factor of 400 relative to an uncompensated K magnetometer. The transient decay time is much faster than the nuclear spin relaxation time due to dynamic spin damping [14]. For a sinusoidally oscillating magnetic field at a frequency ω , the largest sensitivity comes from the B_x field and is suppressed by $\omega/(\gamma_n B^n)$. The measured response of the comagnetometer to oscillating magnetic fields is shown in Fig. 5.

The comagnetometer also effectively suppresses magnetic field gradients even though alkali-metal and noble-gas polarizations have different spatial distributions. The polarization of the noble gas is constant in absolute value and parallel to the local direction of the magnetic field because the noble-gas diffusion rate R_D satisfies the relationship $\gamma_n B^n \gg R_D \gg R_{sd}^n$. Thus, the nuclear magnetization largely cancels the nonuniform external field point by point. The imperfections of this cancellation are expected to be on the order of 10^{-3} . We measured the sensitivity to first-order magnetic field gradients and obtained suppression factors of 500 to 5000 relative to $S_g = \gamma_e |\nabla B| a P_z^e / R_{tot}$, where a is the radius of the cell.

The fundamental limit on gyroscope sensitivity is due to spin projection noise. We performed a quantum trajectory

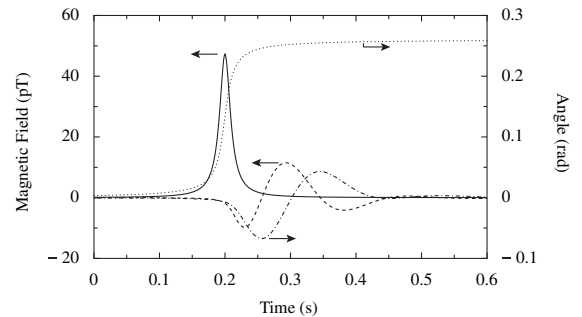


FIG. 4. Response of the comagnetometer (dashed line) to a magnetic field transient (solid line), plotted against the left axis. The total rotation angle (dash-dotted line), proportional to the integral of the comagnetometer signal, is much smaller than the expected rotation angle for an uncompensated K magnetometer (dotted line), plotted against the right axis.

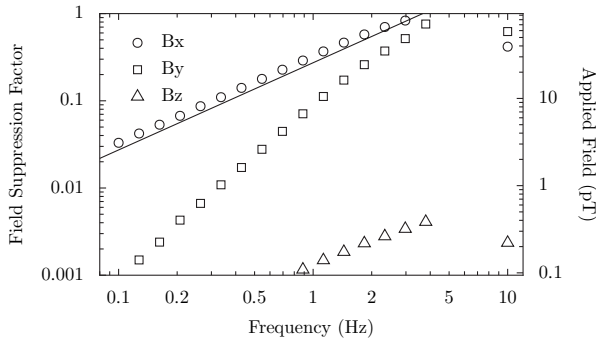


FIG. 5. Suppression of the comagnetometer response to uniform oscillating fields in the \hat{x} , \hat{y} , and \hat{z} directions relative to the signal expected from an uncompensated magnetometer. The field sensitivity is highest in the \hat{x} direction and agrees with theoretical predictions (solid line).

simulation of the coupled spin system (1) to show that for most parameters the measurement uncertainty is dominated by the alkali-metal spins. The rotational uncertainty per unit bandwidth is given by $\delta\Omega_y = (\gamma_n/\gamma_e) \times [Q(P^e)R_{\text{tot}}/nV]^{1/2}$ where n is the density of alkali-metal atoms and V is the measurement volume. ^{21}Ne gives the best fundamental sensitivity and suppression of systematic effects because it has a small gyromagnetic ratio γ_n , 10 times smaller than ^3He . Using the K- ^{21}Ne spin relaxation cross section measured in [19], we estimate the fundamental sensitivity to be $2 \times 10^{-10} \text{ rad s}^{-1} \text{ Hz}^{-1/2}$ for a measurement volume of 10 cm^3 , K density of 10^{14} cm^{-3} , and ^{21}Ne density of $6 \times 10^{19} \text{ cm}^{-3}$. Detection of the off-resonant optical rotation can approach the spin projection noise even with imperfect detectors by making a quantum-non-demolition measurement of the alkali-metal spin in an optically thick vapor [20].

For comparison, gyroscopes based on the Sagnac effect have achieved sensitivities of $2 \times 10^{-10} \text{ rad s}^{-1} \text{ Hz}^{-1/2}$ using a ring laser with an enclosed area of 1 m^2 [21] and $6 \times 10^{-10} \text{ rad s}^{-1} \text{ Hz}^{-1/2}$ using an atomic interferometer with a path length of 2 m [22]. More compact atomic interferometers using cold atoms are presently being developed with a projected shot-noise sensitivity of $3 \times 10^{-8} \text{ rad s}^{-1} \text{ Hz}^{-1/2}$ [4] and $2 \times 10^{-9} \text{ rad s}^{-1} \text{ Hz}^{-1/2}$ [23]. Compact state-of-the-art fiber-optic gyroscopes have a reported sensitivity of $2 \times 10^{-8} \text{ rad s}^{-1} \text{ Hz}^{-1/2}$ [24]. Thus, the gyroscope described here is promising as a compact rotation sensor that can rival existing technologies. Its relative simplicity makes it amenable to miniaturization with techniques developed for atomic clocks [25]. Small size and fast transient response may also allow reduction of long-term drifts using active rotation techniques [26].

In conclusion, we have described the operation and performance of a K- ^3He comagnetometer gyroscope. It has a high short term sensitivity with a small measurement

volume and is insensitive to external perturbations. Further improvement is possible by switching to ^{21}Ne gas. The comagnetometer is also a promising tool in searches for new physics effects that couple to electron and nuclear spins not in proportion to their magnetic moments.

We thank Tom Jackson, Igor Savukov, Charles Sule, and Saeed Paliwal for assistance in the lab. This work was supported by NASA, NSF, a NIST Precision Measurement Grant, and the Packard Foundation.

- [1] G.E. Stedman, Rep. Prog. Phys. **60**, 615 (1997).
- [2] I.A. Andronova and G.B. Malykin, Phys. Usp. **45**, 793 (2002).
- [3] T.L. Gustavson, P. Bouyer, and M.A. Kasevich, Phys. Rev. Lett. **78**, 2046 (1997).
- [4] F. Yver-Leduc *et al.*, J. Opt. B **5**, S136 (2003).
- [5] O. Avenel, Yu. Mukharsky, and E. Varoquaux, J. Low Temp. Phys. **135**, 745 (2004).
- [6] K.F. Woodman, P.W. Franks, and M.D. Richards, Journal of Navigation **40**, 366 (1987).
- [7] S. Buchman *et al.*, Physica B (Amsterdam) **280**, 497 (2000).
- [8] B.C. Grover, E. Kanegsberg, J.G. Mark, R.L. Meyer, U.S. Patent No. 4 157 495, 1979.
- [9] I.A. Greenwood, U.S. Patent No. 4 147 974, 1979.
- [10] M.A. Rosenberry and T.E. Chupp, Phys. Rev. Lett. **86**, 22 (2001).
- [11] D. Bear, R.E. Stoner, R.L. Walsworth, V.A. Kostelecký, and C.D. Lane, Phys. Rev. Lett. **85**, 5038 (2000); **89**, 209902(E) (2002).
- [12] I.K. Kominis, T.W. Kornack, J.C. Allred, and M.V. Romalis, Nature (London) **422**, 596 (2003).
- [13] I.M. Savukov and M.V. Romalis, Phys. Rev. A **71**, 023405 (2005).
- [14] T.W. Kornack and M.V. Romalis, Phys. Rev. Lett. **89**, 253002 (2002).
- [15] T.W. Kornack and M.V. Romalis, in *Proceedings of the Third Meeting on CPT and Lorentz Symmetry*, edited by A. Kostelecký (World Scientific, Singapore, 2004), p. 57.
- [16] S.R. Schaefer *et al.*, Phys. Rev. A **39**, 5613 (1989).
- [17] T.G. Walker, Phys. Rev. A **40**, 4959 (1989).
- [18] W. Happer and B.S. Mathur, Phys. Rev. **163**, 12 (1967).
- [19] F.A. Franz and C. Volk, Phys. Rev. A **26**, 85 (1982).
- [20] M. Auzinsh *et al.*, Phys. Rev. Lett. **93**, 173002 (2004).
- [21] G.E. Stedman, K.U. Schreiber, and H.R. Bilger, Classical Quantum Gravity **20**, 2527 (2003).
- [22] T.L. Gustavson, A. Landragin, and M.A. Kasevich, Classical Quantum Gravity **17**, 2385 (2000).
- [23] C. Jentsch, T. Müller, E.M. Rasel, and W. Ertmer, Gen. Relativ. Gravit. **36**, 2197 (2004).
- [24] S.J. Sanders, L.K. Strandjord, and D. Mead, in *15th Optical Fiber Sensors Conference Tech. Digest* (IEEE, Portland, 2002), p. 5.
- [25] S. Knappe *et al.*, Appl. Phys. Lett. **85**, 1460 (2004).
- [26] K.M. Hays *et al.*, in *IEEE Position and Navigation Symposium* (IEEE, Palm Springs, 2002), p. 179.